MOLECULAR IMAGING AND BIOLOGY

Mol Imaging Biol (2019) 21:818–824
DOI: 10.1007/s11307-018-01309-y

Published Online: 7 January 2019

BRIEF ARTICLE

Feasibility of Hyperfunctioning Parathyroid Gland Localization Using [^{18}F]fluciclovine PET/CT

Akinyemi A. Akintayo,[1] O. A. Abiodun-Ojo,[1] C. Weber,[2] J. Sharma,[2] C. Cohen,[3] G. Sica,[3] R. Halkar,[1] M. M. Goodman,[1] D. M. Schuster[1]

[1]*Department of Radiology and Imaging Sciences, Division of Nuclear Medicine and Molecular Imaging, Emory University Hospital, 1364 Clifton Road, Atlanta, GA, USA*
[2]*Department of Surgery, Emory University, Atlanta, GA, USA*
[3]*Department of Pathology and Laboratory Medicine, Emory University, Atlanta, GA, USA*

Abstract

Purpose: To evaluate the ability of anti-1-amino-3-anti-1-amino-3-[^{18}F]fluorocyclobutane-1-carboxylic acid ([^{18}F]fluciclovine) positron emission tomography/X-ray computed tomography (PET/CT) in comparison to Technetium-99m 2-methoxy isobutyl isonitrile ([^{99m}Tc]sestamibi) single-photon emission computed tomography/CT (SPECT/CT) for the localization of hyperfunctioning parathyroid glands in patients with hyperparathyroidism.

Procedures: Four patients with hyperparathyroidism underwent 60-minutes sequential neck and thorax PET/CT after [^{18}F]fluciclovine (352 ± 28 MBq) injection. Lesion uptake and target-to-background ratios (TBR) were compared with [^{99m}Tc]sestamibi (798 ± 27 MBq) SPECT/CT in the same patient.

Results: Both techniques detected 4/5 hyperfunctioning parathyroid glands identified at surgery. The highest [^{18}F]fluciclovine uptake and TBRs were at 5–9 min with rapid washout. [^{99m}Tc]sestamibi had significantly higher TBRs compared with [^{18}F]fluciclovine (5–9 min) for blood pool (10.9 ± 4.7 *vs* 1.3 ± 0.6; $p < 0.01$) and reference muscle backgrounds (5.8 ± 3.0 *vs* 1.7 ± 0.6; $p < 0.01$), with non-significant trend for thyroid tissue background (1.3 ± 0.5 *vs* 1.1 ± 0.5; $p = 0.73$).

Conclusion: Hyperfunctioning parathyroid glands can be detected on [^{18}F]fluciclovine PET/CT at early imaging, but conspicuity (TBR) is better with [^{99m}Tc]sestamibi. [^{18}F]fluciclovine PET/CT does not seem promising in the detection of hyperfunctioning parathyroid glands.

Key words: Hyperfunctioning parathyroid gland, [^{18}F]fluciclovine, PET/CT, SPECT/CT, [^{99m}Tc]sestamibi

Introduction

Hyperfunctioning parathyroid glands are common benign endocrine tumors. Hyperparathyroidism is usually caused by hyperfunctioning parathyroid glands (parathyroid adenoma and parathyroid hyperplasia). Solitary adenomas are the leading cause of primary hyperparathyroidism [1]. The pathophysiologic effects of these hyperfunctioning parathyroid glands are related to hypercalcemia with elevated parathyroid hormone levels. These cause significant multisystem morbidity, including worsening of arteriosclerotic disease, hypertension, cardiac arrhythmias, change in

Correspondence to: Akinyemi Akintayo; *e-mail:* aakint2@emory.edu

mentation, and gastrointestinal pain and ulcers. Surgery is the only effective management for primary hyperparathyroidism. Therefore, it is desirable to have non-invasive preoperative imaging techniques which adequately identify hyperfunctioning parathyroid gland for surgical planning, especially with the advent of minimally invasive parathyroidectomy [2, 3].

Conventional imaging techniques, X-ray computerized tomography (CT) [4], magnetic resonance imaging (MRI) [5, 6], and ultrasonography [7], have been utilized for detecting hyperfunctioning parathyroid gland, but each has its own limitations. Molecular imaging with Technetium-99m 2-methoxy isobutyl isonitrile ([99mTc]sestamibi) has been used widely for parathyroid imaging due to its higher uptake in hyperfunctioning parathyroid gland in comparison to normal parathyroid tissue [8]. Single-photon emission computed tomography/X-ray computed tomography (SPECT/CT) enhances the ability of [99mTc]sestamibi to detect and localize hyperfunctioning parathyroid gland by improving contrast resolution. The sensitivity of [99mTc]sestamibi in preoperative localization of hyperfunctioning parathyroid gland was reported in a systematic review as 88 % in solitary lesions [9], but the sensitivity is lower for smaller lesions [10] and multiple adenomas [9, 11].

Recent studies have shown that imaging with positron emission tomography (PET) using the radiotracers carbon-11 choline ([11C]choline) [12, 13], [18F]fluorocholine ([18F]choline) [14, 15], and [11C]-methyl-methionine ([11C]MET) [16, 17] have shown promising results in the detection of hyperfunctioning parathyroid gland. PET has better imaging characteristics compared to SPECT; improved spatial resolution enables detection of smaller lesions. Meta-analysis of PET using these radiotracers concluded that while [18F]]choline shows promise, [11C]MET is considered a good adjunctive imaging modality for hyperfunctioning parathyroid gland [18].

[18F]fluciclovine is a synthetic L-leucine analog approved by the Food and Drug Administration (FDA) for detection of recurrent prostate cancer. Parathyroid hormone is a peptide hormone with a long helical dimer containing ten leucine residues. Amino acid radiotracers such as methionine have uptake within hyperfunctioning parathyroid glands, probably due to upregulation of amino acid transporters in these glands. Hence, we hypothesized that hyperfunctioning parathyroid cells would take up the amino acid radiotracer, [18F]fluciclovine, and therefore, it could be used to improve detection of hyperfunctioning parathyroid hyperplasia/adenoma.

We carried out this feasibility study in humans to evaluate the ability of [18F]fluciclovine PET/CT in comparison to [99mTc Tc]sestamibi to detect and localize hyperfunctioning parathyroid glands in patients with hyperparathyroidism. We also set out to analyze the uptake kinetics of [18F]fluciclovine in hyperfunctioning parathyroid glands.

Materials and Methods

This feasibility pilot study was approved by the institutional review board and was performed in compliance with Health Insurance Portability and Accountability Act (HIPPA).

Patient Selection

The inclusion criteria for this study were patients ≥ 18 years old that had clinical and biochemical evidence of primary hyperparathyroidism and were able to give informed consent. Patients with secondary hyperparathyroidism were excluded. Four patients with primary hyperparathyroidism were recruited for the study after obtaining written informed consents. All participants underwent [18F]fluciclovine PET/CT and [99mTc]sestamibi scans.

Imaging Protocol

[99mTc]Sestamibi Planar (Early and Delayed) and Delayed SPECT/CT Imaging Standard of care dual phase (early and delayed) planar images were obtained. Anterior planar images of the neck and thorax were acquired at 10 min (early images) and 2–2.5 h (delayed images) after intravenous administration of 798 ± 27 MBq [99mTc]sestamibi with the patient in supine position, neck extended, and shoulders supported by a pillow. Forty-five minutes after the early planar images, SPECT/CT of the neck and thorax was obtained. Images were acquired using a Siemens-Healthineer Symbian T-series (6 slice) SPECT/CT (Siemens-Healthineer, Malvern, PA). Acquisition using low-energy high-resolution collimator was at 180° gantry rotation with 45 stops per head and 30 s per stop. Reconstruction was with Flash-3D 16 iteration, 6 subsets, Gaussian 10-mm filter. Attenuation correction was with CT.

[18F]fluciclovine PET/CT Imaging The radiotracer was administered under FDA Investigational New Drug (IND) 72,437 and was synthesized either *via* automated synthesis or the FastLab Cassette System (GE Healthcare). Safety monitoring during the drug infusion was performed, and no adverse events were recorded. All subjects were required to fast for 4 h to normalize their neutral amino acid levels.

PET images were acquired on a GE Discovery DLS 16 slice integrated PET/CT scanner (GE Healthcare, Waukesha, WI). The patient was positioned supine with neck extended and arms placed above the heads. The patient first underwent a low-dose CT scan of the neck and thorax, down to the carina (120 kV, automA, maximum 160 mA) without oral or intravenous contrast, for anatomic correlation and attenuation correction of emission data (approximately 1 min). [18F]fluciclovine was administered as an intravenous bolus injection (352 ± 28 MBq) over 1 min, then images were obtained starting 4 min post-injection. PET scans of the neck and thorax down to the carina was carried out in two

Table 1. Demographic and clinical variables

Serial no.	Age (years)	Sex	PTH (pg/ml)		Location	Size (cm)	Weight (g)	Histology
			Pre-op	Post-op				
1	53	F	336	44	Left upper parathyroid gland	1.5 × 0.9 × 0.5	0.35	Adenoma
2	64	M	522	100[a]	Within right thymus	2.2 × 1.5 × 1.0	4.40	Hyperplasia
3	64	F	161	45	a. Left lower parathyroid gland	1.3 × 0.8 × 0.4	0.28	Adenoma
					b. Left upper parathyroid gland[b]	0.2 × 0.2 × 0.1	0.01	Adenoma
4	46	F	213	44	Left lower parathyroid gland	1.5 × 1.1 × 0.4	0.47	Hyperplasia

PTH parathyroid hormone
[a]PTH value on the first post-operative day was 82 pg/ml
[b]Adenoma found only at surgery

consecutive 2.5-min bed positions at sequential time points over 60 min. Images were reconstructed with iterative technique and hardware fused (PET to CT) on a MimVista workstation (MIM Software, Cleveland, OH). Reconstruction parameters were VUE point FX with 3 iterations/24 subsets and 6.4-mm filter cutoff, and reconstructed slice thickness was 3.75 mm.

Image Analysis

All images were interpreted by a board certified nuclear radiologist with over 15 years' experience, blinded to the other imaging study that may have been acquired in the same patient including ultrasound, MR, and/or CT of the neck.

[18F]fluciclovine PET/CT [18F]fluciclovine uptake parameters, maximum and mean standard uptake values (SUVmax, SUVmean), were determined for the suspected hyperfunctioning parathyroid gland, thyroid tissue, muscle (pectoralis major), and blood pool in the aortic arch at each time point. 3D volumes of interest (VOI) of at least 1 cm^3 were utilized for the lesions where possible. In smaller lesions, VOIs were drawn to fit the anatomic lesion. Representative areas on the background utilizing blood pool (aortic arch), muscle (pectoralis), or thyroid tissue were drawn. TBRs (SUVmax hyperfunctioning parathyroid gland/ SUVmean background) were determined for each time point.

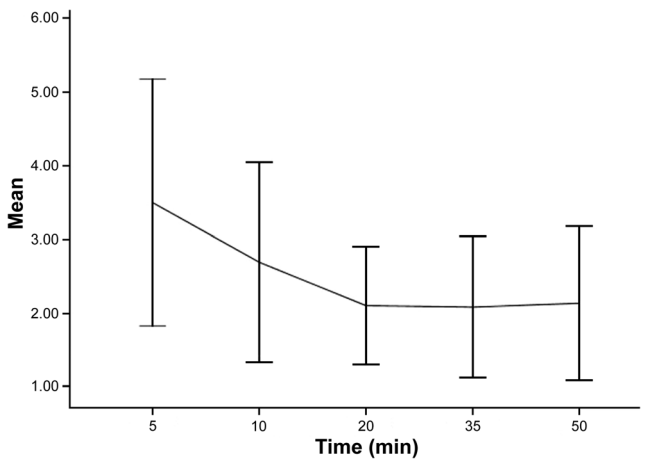

Fig. 1. Time–activity curve for mean SUVmax of hyperfunctioning parathyroid gland on [18]fluciclovine PET/CT. Error bars ± 1 SD.

[99mTc]Sestamibi Planar (Early and Delayed) and Delayed SPECT/CT [99mTc]sestamibi scans were reported per clinical routine. Subsequent to analysis of the PET/CT, VOIs were drawn on the same regions as in the [18F]fluciclovine PET/CT for each patient. [99mTc Tc]sestamibi SPECT/CT TBRs (maximum counts per minute of the hyperfunctioning parathyroid gland/ mean counts per minute of the background) were compared with TBRs for [18F]fluciclovine PET/CT in the same patient.

Surgical Correlation

All the patients in this study had surgical resection of hyperfunctioning parathyroid gland. Parathyroid hormone levels were obtained after resection. Histopathologic confirmation of parathyroid adenoma or hyperplasia was reference standard for truth.

Data Analysis

Data entry was done with Microsoft Excel (Microsoft, Redmond, WA), and data was analyzed using SPSS version 23 (IBM, Armonk, NY). Descriptive analysis was carried out, and mean ± SD was reported as appropriate. Difference in means of uptake parameters for [18F]fluciclovine PET compared with [99mTc]sestamibi was determined using *t* test. Statistical significance was set at $p < 0.05$.

Results

Demographics

Four patients, three females and one male, were included in this study. As noted in Table 1, the average age of the

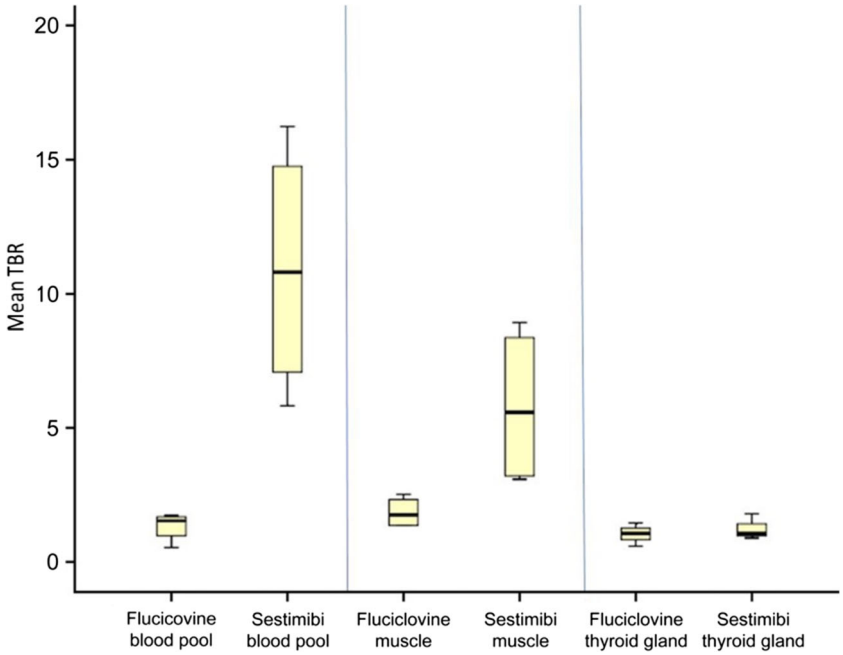

Fig. 2. Mean target-to-background ratios for [18F]fluciclovine PET/CT at 5–9 min *vs* [99mTc]sestamibi delayed SPECT/CT using the reference backgrounds (aortic blood pool, pectoralis muscle, and thyroid gland).

patients was 57 ± 9 years (range 46–64 years). The average preoperative parathyroid hormone level was 308 ± 160 pg/ml (normal range 12–88 pg/ml) and serum calcium was 10 ± 0.6 mg/dl (normal range 8.6–10.3 mg/dl). The average interval between the [99mTc]sestamibi scan and the [18F]fluciclovine PET scan was 35 ± 20 days, while the average time between the [18F]fluciclovine PET scan and surgery was 14 ± 10 days.

Target Localization

Both modalities showed 100 % concordance in the detection and localization of hyperfunctioning parathyroid gland. The highest [18F]fluciclovine SUVs were at the 5 min time point with rapid washout (Fig. 1). [99mTc]sestamibi had significantly higher TBRs compared with [18F]fluciclovine (5–9 min) for blood pool (10.9 ± 4.7 *vs* 1.3 ± 0.6; $p < 0.01$) and pectoralis muscle (5.8 ± 3.0 *vs* 1.7 ± 0.6; $p < 0.01$) backgrounds with a non-significant trend for thyroid tissue background (1.3 ± 0.5 *vs* 1.1 ± 0.5; $p = 0.73$) (Fig. 2).

Table 2 shows the comparison of the uptake parameters and target-to-background ratios of the hyperfunctioning parathyroid glands on [18F]fluciclovine PET and [99mTc]sestamibi scans. Figure 3 is a representative image comparing tumor conspicuity between both techniques. Histology of a representative excised hyperfunctioning parathyroid gland is shown on Fig. 4.

Surgical Findings

Five hyperfunctioning parathyroid glands were identified in four patients, including one at an ectopic site within the thymus. Sizes of the identified hyperfunctioning parathyroid glands ranged from 0.2 to 2.2 cm in the longest diameter, and the weight ranged from 0.01 to 4.4 g. The small adenoma (2 × 2 mm; weight 0.01 g) identified only at

Table 2. Mean SUVmax and target-to-background ratios

	Mean SUVmax ± SD (PET/CT)					CPM (SPECT/CT)
	5–9 min	10–14 min	20–24 min	25–39 min	50–54 min	45 min
Hyperfunctioning parathyroid gland	3.5 ± 1.7	2.6 ± 1.2	2.1 ± 0.8	2.1 ± 1.0	2.2 ± 1.0	661.5 ± 395.7
Reference background	Target-to-background ratios					
Muscle (pectoralis)	1.7 ± 0.6	1.5 ± 0.5	1.0 ± 0.3	0.8 ± 0.6	0.7 ± 0.5	5.8 ± 3.0
Thyroid gland[a]	1.1 ± 0.5	1.4 ± 0.6	1.1 ± 0.4	1.4 ± 0.6	1.4 ± 0.6	1.3 ± 0.5
Blood pool (aorta)	1.3 ± 0.6	1.3 ± 0.5	1.4 ± 0.3	1.4 ± 0.5	1.6 ± 0.6	10.9 ± 4.7

CPM counts per minute
[a]Mean values for the thyroid gland were for three patients

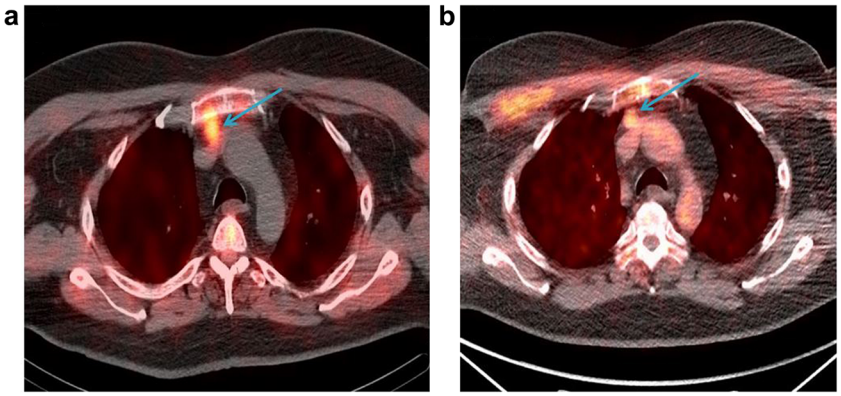

Fig. 3. Detection of hyperfunctioning parathyroid gland using [99mTc]sestamibi delayed SPECT/CT *vs* [18F]fluciclovine PET/CT. **a** Fused image of [99mTC]sestamibi delayed SPECT/CT in a 64-year-old patient with hyperparathyroidism. Hypercellular parathyroid gland is indicated with the blue arrow (respiratory movement detected). TBR (blood pool) was 16.2 and TBR (muscle) was 7.8. **b** Fused image of [18F]fluciclovine PET/CT in a 64-year-old patient with hyperparathyroidism. Hypercellular parathyroid gland is indicated with the blue arrow (respiratory movement detected). TBR (blood pool) was 1.6 and TBR (muscle) was 1.4.

surgery and confirmed histologically was not detected by either modality. Hence, the detection rate for both modalities was 4/5 (80 %).

After surgical resection of the hyperfunctioning parathyroid glands, the post-operative parathyroid hormone levels decreased to normal with a median reduction of 80 % (range 72–87 %). Mean parathyroid hormone level post-operatively was 58 ± 28 pg/ml. Histopathology confirmed hyperfunctioning parathyroid gland (three parathyroid adenomas and two parathyroid hyperplasia) in all patients.

Discussion

We set out to determine the feasibility of detection and localization of hyperfunctioning parathyroid gland in patients with hyperparathyroidism using [18F]fluciclovine PET/CT. In this small series, we found that hyperfunctioning parathyroid glands can be detected on [18F]fluciclovine PET/CT at early imaging with maximum TBR at 5–9 min after [18F]fluciclovine injection but with rapid washout. Although, the detection rate of [18F]fluciclovine was comparable to [99mTc]sestamibi SPECT/CT, with 4/5(80 %)

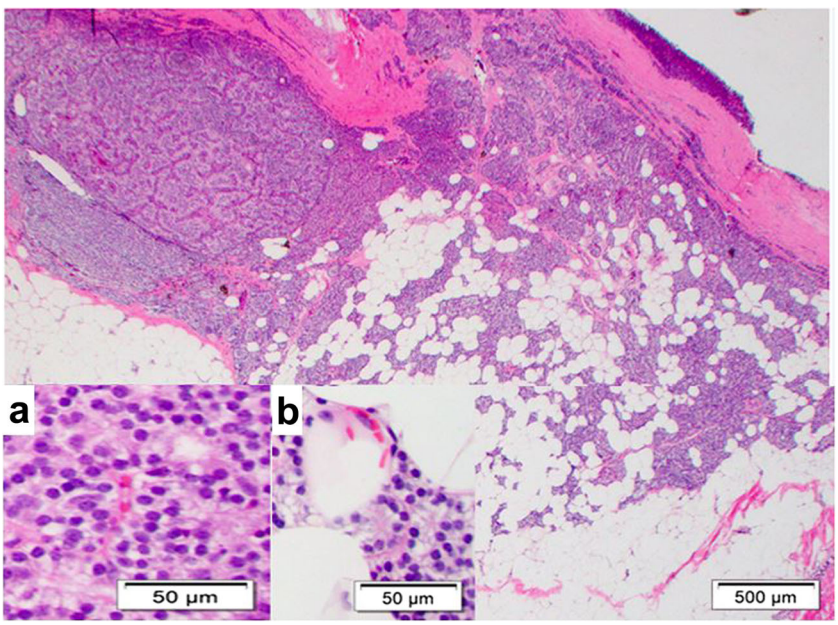

Fig. 4. Hematoxylin and eosin–stained slides of right thymic hyperfunctioning parathyroid gland (2.2 cm) with variable cellularity. The gland was excised with attached atrophic thymic gland tissue (not shown). **a** High magnification of hypercellular area. **b** High magnification of less cellular area.

detection rate and 100 % concordance between both techniques, tumor conspicuity (TBR) was significantly better with [99mTc]sestamibi SPECT/CT.

The detection rate of 80 % for [99mTc]sestamibi is consistent with the reports on the diagnostic ability of [99mTc]sestamibi for solitary adenoma from previous studies [9]. Inability to detect the smaller (2 × 2 mm) lesion by both techniques is not surprising as this size is significantly below the physical detection rates of both techniques [9]. Smaller lesions may be more easily detected with PET, but this was not the case with [18F]fluciclovine.

Commonly, [99mTc]sestamibi SPECT/CT is used as first-line imaging technique to localize hyperfunctioning parathyroid glands [11, 19]. The need for a better and more reliable preoperative imaging technique has informed the use of various functional and anatomical techniques. PET, using various radiotracers, has been studied for use in localization of hyperfunctioning parathyroid tissue. Several studies using 2-deoxy-2-[18F]fluoro-D-glucose in patients with primary hyperparathyroidism to localize hyperfunctioning parathyroid gland have reported conflicting results for sensitivity, as high as 94 % [20] and as low as 0 % [21]. A study evaluating dihydroxy-[18F]fluorophenylalanine ([18F]FDOPA) concluded that it does not have a role in parathyroid imaging [22]. Studies involving methionine have shown promise, and it has been recommended as an adjunct test in [99mTc]sestamibi-negative patients [16, 23] and not a replacement for [99mTc]sestamibi imaging [16, 17].

Both [11C]choline and [18F]flurocholine PET/CT have been reported in a systematic review and meta-analysis to have better detection and imaging quality than [99mTc]sestamibi in the localization of hyperfunctioning parathyroid gland [24]. Studies involving the use of 11C-choline [12, 13] demonstrated higher SUVmax and TBRs to thyroid gland and blood pool backgrounds compared to the values we reported for [18F]fluciclovine. Even at the early time point on [18F]fluciclovine PET/CT, the SUVmax in the hyperfunctioning parathyroid gland and the TBRs are low, making tumor conspicuity poor.

The aim of preoperative localization of hyperfunctioning parathyroid gland is to enable minimal and precise surgical incisions with the goal of achieving cure. Although this series shows that [18F]fluciclovine PET/CT may be able to detect and localize hyperfunctioning parathyroid gland, [99mTc]sestamibi SPECT/CT appears to be a better technique in relation to visualization and conspicuity of the hyperfunctioning parathyroid gland.

The number of patients evaluated is a limitation of our study. Despite much effort, recruitment was difficult and the decision to terminate the study was made after the initial data was analyzed. This small series gives us insight into the feasibility of [18F]fluciclovine PET/CT in the preoperative assessment of a patient with hyperfunctioning parathyroid gland. A larger prospective study will be required to make further conclusions, though [18F]fluciclovine does not seem promising. Also, patients who had negative [99mTc]sestamibi scans were not included in this study; information on the role of [18F]fluciclovine in that group of patients may provide insight to a potential role for [18F]fluciclovine.

Conclusion

In this small series, we found that hyperfunctioning parathyroid glands can be detected on [18F]fluciclovine PET/CT at early imaging but with rapid washout leading to suboptimal imaging. In addition, conspicuity (TBR) of hyperfunctioning parathyroid glands was better with [99mTc]sestamibi compared with [18F]fluciclovine. Although [18F]fluciclovine PET/CT does not seem promising in the detection and localization of [99mTc]sestamibi avid hyperfunctioning parathyroid glands, studies in patients with negative [99mTc]sestamibi scans may be worthwhile to determine if there could be added value of [18F]fluciclovine in this sub-population.

Acknowledgements. We gratefully acknowledge the contributions of Ronald Crowe, RPh, BCNP and the cyclotron/synthesis team from Emory University Center for Systems Imaging.

Compliance with Ethical Standards. This feasibility pilot study was approved by the institutional review board and was performed in compliance with Health Insurance Portability and Accountability Act (HIPPA).

Conflicts of Interest

Emory University and Dr. Mark Goodman are eligible to receive royalties for [18F]fluciclovine. Blue Earth Diagnostics Ltd. provided [18F]fluciclovine synthesis cassettes to Emory University for this project. Although not impacting this study, funding is or has been received from Blue Earth Diagnostics Ltd. and Nihon Medi-Physics Co. Ltd. through the Emory University Office of Sponsored Projects for other clinical trials using FACBC ([18F]fluciclovine).

References

1. Bilezikian JP, Bandeira L, Khan A, Cusano NE (2018) Hyperparathyroidism. Lancet 391:168–178
2. Udelsman R, Lin Z, Donovan P (2011) The superiority of minimally invasive parathyroidectomy based on 1650 consecutive patients with primary hyperparathyroidism. Ann Surg 253:585–591
3. Kunstman JW, Kirsch JD, Mahajan A, Udelsman R (2013) Clinical review: parathyroid localization and implications for clinical management. J Clin Endocrinol Metab 98:902–912
4. Kluijfhout WP, Pasternak JD, Beninato T, Drake FT, Gosnell JE, Shen WT, Duh QY, Allen IE, Vriens MR, de Keizer B, Hope TA, Suh I (2017) Diagnostic performance of computed tomography for parathyroid adenoma localization; a systematic review and meta-analysis. Eur J Radiol 88:117–128
5. Lopez Hanninen E, Vogl TJ et al (2000) Preoperative contrast-enhanced MRI of the parathyroid glands in hyperparathyroidism. Investig Radiol 35:426–430
6. Gotway MB, Reddy GP, Webb WR, Morita ET, Clark OH, Higgins CB (2001) Comparison between MR imaging and 18Tc MIBI scintigraphy in the evaluation of recurrent of persistent hyperparathyroidism. Radiology 218:783–790
7. Stern S, Tzelnick S, Mizrachi A, Cohen M, Shpitzer T, Bachar G (2018) Accuracy of neck ultrasonography in predicting the size and location of parathyroid adenomas. Otolaryngol Head Neck Surg 159:968–972. https://doi.org/10.1177/0194599818792236

8. Mitchell BK, Merrell RC, Kinder BK (1995) Localization studies in patients with hyperparathyroidism. Surg Clin North Am 75:483–498
9. Ruda JM, Hollenbeak CS, Stack BC Jr (2005) A systematic review of the diagnosis and treatment of primary hyperparathyroidism from 1995 to 2003. Otolaryngol Head Neck Surg 132:359–372
10. Biertho LD, Kim C, Wu HS, Unger P, Inabnet WB (2004) Relationship between sestamibi uptake, parathyroid hormone assay, and nuclear morphology in primary hyperparathyroidism. J Am Coll Surg 199:229–233
11. Chien D, Jacene H (2010) Imaging of parathyroid glands. Otolaryngol Clin N Am 43:399–415
12. Orevi M, Freedman N, Mishani E, Bocher M, Jacobson O, Krausz Y (2014) Localization of parathyroid adenoma by ^{11}C-choline PET/CT: preliminary results. Clin Nucl Med 39:1033–1038
13. Parvinian A, Martin-Macintosh EL, Goenka AH, Durski JM, Mullan BP, Kemp BJ, Johnson GB (2018) ^{11}C-choline PET/CT for detection and localization of parathyroid adenomas. AJR Am J Roentgenol 210:418–422
14. Beheshti M, Hehenwarter L, Paymani Z, Rendl G, Imamovic L, Rettenbacher R, Tsybrovskyy O, Langsteger W, Pirich C (2018) ^{18}F-Fluorocholine PET/CT in the assessment of primary hyperparathyroidism compared with ^{99m}Tc-MIBI or ^{99m}Tc-tetrofosmin SPECT/CT: a prospective dual-centre study in 100 patients. Eur J Nucl Med Mol Imaging 45:1762–1771
15. Quak E, Blanchard D, Houdu B, le Roux Y, Ciappuccini R, Lireux B, de Raucourt D, Grellard JM, Licaj I, Bardet S, Reznik Y, Clarisse B, Aide N (2018) F18-choline PET/CT guided surgery in primary hyperparathyroidism when ultrasound and MIBI SPECT/CT are negative or inconclusive: the APACH1 study. Eur J Nucl Med Mol Imaging 45:658–666
16. Weber T, Gottstein M, Schwenzer S, Beer A, Luster M (2017) Is C-11 methionine PET/CT able to localise sestamibi-negative parathyroid adenomas? World J Surg 41:980–985
17. Oksuz MO, Dittmann H, Wicke C et al (2011) Accuracy of parathyroid imaging: a comparison of planar scintigraphy, SPECT, SPECT-CT, and C-11 methionine PET for the detection of parathyroid adenomas and glandular hyperplasia. Diagn Interv Radiol 17:297–307
18. Kluijfhout WP, Pasternak JD, Drake FT, Beninato T, Gosnell JE, Shen WT, Duh QY, Allen IE, Vriens MR, de Keizer B, Pampaloni MH, Suh I (2016) Use of PET tracers for parathyroid localization: a systematic review and meta-analysis. Langenbeck's Arch Surg 401:925–935
19. Bilezikian JP, Khan AA, Potts JT Jr (2009) Guidelines for the management of asymptomatic primary hyperparathyroidism: summary statement from the third international workshop. J Clin Endocrinol Metab 94:335–339
20. Neumann DR, Esselstyn CB Jr, MacIntyre WJ et al (1994) Primary hyperparathyroidism: preoperative parathyroid imaging with regional body FDG PET. Radiology 192:509–512
21. Sisson JC, Thompson NW, Ackerman RJ, Wahl RL (1994) Use of 2-[F-18]-fluoro-2-deoxy-D-glucose PET to locate parathyroid adenomas in primary hyperparathyroidism. Radiology 192:280
22. Lange-Nolde A, Zajic T, Slawik M, Brink I, Reincke M, Moser E, Hoegerle S (2006) PET with ^{18}F-DOPA in the imaging of parathyroid adenoma in patients with primary hyperparathyroidism. A pilot study. Nuklearmedizin 45:193–196
23. Hayakawa N, Nakamoto Y, Kurihara K, Yasoda A, Kanamoto N, Miura M, Inagaki N, Togashi K (2015) A comparison between 11C-methionine PET/CT and MIBI SPECT/CT for localization of parathyroid adenomas/hyperplasia. Nucl Med Commun 36:53–59
24. Treglia G, Piccardo A, Imperiale A, Strobel K, Kaufmann PA, Prior JO, Giovanella L (2018) Diagnostic performance of choline PET for detection of hyperfunctioning parathyroid glands in hyperparathyroidism: a systematic review and meta-analysis. Eur J Nucl Med Mol Imaging. https://doi.org/10.1007/s00259-018-4123-z